# Power Dependence of Distributed Cavity Phase-Induced Frequency Biases in Atomic Fountain Frequency Standards

Steven R. Jefferts, *Member, IEEE*, Jon H. Shirley, Neil Ashby, Eric A. Burt, *Member, IEEE*, and G. John Dick

***Abstract*—We discuss the implications of using high-power microwave tests in a fountain frequency standard to measure the frequency bias resulting from distributed cavity-phase shifts. We develop a theory which shows that the frequency bias from distributed cavity phase depends on the amplitude of the microwave field within the cavity. The dependence leads to the conclusion that the frequency bias associated with the distributed cavity phase is typically both misestimated and counted twice within the error budget of fountain frequency standards.**

## I. Introduction

The subject of frequency shifts in atomic frequency standards caused by distributed cavity phase is not new; it goes back to the earliest days of the thermal beam standards [1], [2] and has been the subject of continuing work both theoretical and experimental over the last 50 years [3]–[5]. Laser-cooled fountain frequency standards pose significantly different problems with respect to distributed cavity phase than the thermal beam standards. This is due to both the very different microwave structure used in fountains as well as the very narrow velocity distribution that allows test operation at microwave power significantly higher than in normal operation. Observations of power-dependent frequency shifts due to tilting of a short atomic fountain that are related to the work presented here have been made by the group at the Paris Observatory (Systemes de Reference Temps Espace) (SYRTE) [6].

The analysis of the phase of the microwave field within the microwave cavities used in cold atom fountain frequency standards has been the subject of a large body of work. DeMarchi and collegues [7]–[9] provided the seminal contributions of proving the correspondence between the phase and power flows within the microwave cavity, identifying the preferred cavity configuration and modeling the phase of the microwave field within the cavity. Full three-dimensional analyses of the microwave field within the cavity have been completed by several authors [10]–[14]. In many of the studies, large phase excursions are predicted. At least one paper [12] has used these phase excursions to predict frequency shifts as a result of distributed cavity phase in the $\delta f/f \simeq 10^{-16}$ range, outside the current value assigned in the error budget of our fountain-type primary frequency standard. The size of the frequency error caused by the distributed cavity phase is estimated in National Institute of Standards and Technology (NIST)-F1 as $\delta f/f \leq 1 \times 10^{-17}$. The theory presented here allows the direct experimental measurement of the frequency shift at the $\delta f/f \approx 1 \times 10^{-16}$ level, thus discriminating between various estimates of the frequency shift in the NIST fountain.

We begin by briefly reviewing the microwave field within a resonant cavity and recalling various properties of the microwave field and its phase. We then solve the Schrödinger equation for a two-level atom in the case in which the field within the microwave cavity has both real and imaginary parts, which is the case required to understand the distributed cavity phase shift. We then examine the power dependence of the frequency bias caused by distributed cavity phase. The Appendix presents both numerical and analytic integrations of the Bloch vector formulation that agree quite well with the analytic solution of the Schrödinger equation, which we now describe.

## II. Microwave Cavities and Phase

The typical configuration of the microwave cavity, shown schematically in Fig. 1, in cesium (and rubidium) fountain frequency standards is a cylindrical cavity resonating in the $TE_{011}$ mode at the hyperfine frequency of the atom, 9.193 GHz in the case of cesium. The "z-axis" of the cavity is nominally aligned with the gradient of the gravitational potential, and atoms enter and leave the cavity via below-cutoff waveguides. This form of cavity, as described by Vecchi and DeMarchi [8], has the crucial property of allowing below cutoff cylindrical waveguides of relatively large diameter ($2r_a \sim 1$ cm) for atoms to enter and leave the cavity without unduly influencing the $TE_{011}$ mode of the cavity, and thereby causing large phase gradients in the microwave field. To lowest order the field

Manuscript received August 31, 2004; accepted April 25, 2005. Part of the research described in this paper was carried out at the National Institute of Standards and Technology (NIST) and is not subject to U.S. copyright. Part of the research described in this document was carried out at the Jet Propulsion Laboratory, California Institute of Technology, under a contract with the National Aeronautics and Space Administration.

S. R. Jefferts, J. H. Shirley, and N. Ashby are with the National Institute of Standards and Technology, Time and Frequency Division, Boulder, CO 80305 (e-mail: jefferts@boulder.nist.gov).

E. A. Burt and G. J. Dick are with the Jet Propulsion Laboratory, California Institute of Technology, Pasadena, CA 91109.

0885–3010/$20.00 © 2005 IEEE

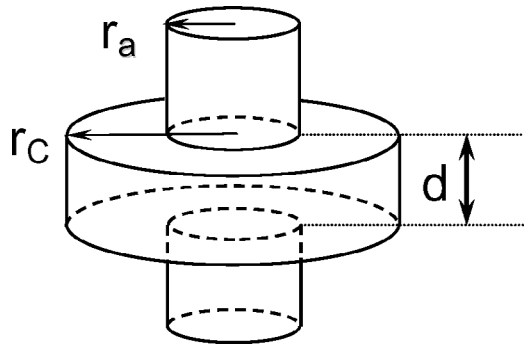


Fig. 1. A schematic of the $TE_{011}$ mode cylindrical cavity showing the principal dimensions. In the NIST-F1 cavity that is resonant at 9.193 GHz, $r_C = 3.00$ cm, $r_a$, the radius of the below cutoff waveguides is 0.50 cm, and $d$ the cavity height is 2.2 cm. The cavity has four symmetrically placed feeds on the midplane and an unloaded $Q$ of 22,500. The loaded $Q$ is also 22,500 as a result of severe undercoupling (the insertion loss of the cavity in transmission is $\approx$30 dB).

within the cavity is describable as purely TE ($E_Z \equiv 0$), and all field components are derivable from the longitudinal magnetic field $H_z(x, y)$ [15]. Under these assumptions, and using a slight extension and modification of the notation of Khursheed *et al.* in [9], the longitudinal field can be written as:

$$H_Z(x, y, z) = |H(x, y)|\, e^{i\varphi(x,y)} f(z), \tag{1}$$

where $\varphi(x, y)$ is the distributed cavity phase under discussion here and $f(z)$ describes the longitudinal variation of $H_Z$. The expression for the real part of the field within the cavity is given (with a change to cylindrical coordinates $\rho$, $\phi$ and $z$) to lowest order by:

$$\mathrm{Re}\,[H_Z(\rho, \phi, z)] = \left(\frac{\pi}{2}\right) H_0 J_0 \left(\frac{p'_{0,1}\rho}{r_C}\right) \sin\left(\frac{\pi z}{d}\right), \tag{2}$$

where $p'_{n,m}$ is defined as the $m^{\text{th}}$ solution of $(dJ_n(x)/dx) = 0$, $r_C$ is the radius of the cavity, $d$ is the height, and $\pi H_0/2$ is the field amplitude at the center of the cavity (see Fig. 1 and [15]). The cavity phase is defined by the relation:

$$\varphi \equiv \tan^{-1}\left(\frac{\mathrm{Im}\,(H_Z)}{\mathrm{Re}\,(H_Z)}\right), \tag{3}$$

where the real part of $H_Z$ is approximated by (2) and the imaginary part is, roughly, approximated by:

$$\mathrm{Im}\,(H_Z) = \frac{\pi H_0}{2Q}\left[\left(1 + \left(\frac{\rho}{r_C}\right)^2 + \left(\frac{\rho}{r_C}\right)^4 \cos 4\phi\right)\left(\frac{z}{d} - \frac{1}{2}\right)^2\right], \tag{4}$$

where $Q$ is the quality factor of the cavity. The second term in (4) comes from power flows to the walls from the standing mode of the field. The third term comes from power flows associated with the four-feed structure of the particular cavity investigated here [10]. The terms proportional to $\rho/r_C$ and $z/d$ should be small for a symmetric, well constructed cavity and are neglected here. The overall cavity phase has been set equal to zero at the geometric center of the cavity, and the various coefficients of the expansion have all been set equal to one.

Several things can be seen by inspection of (1)–(4). The first is that the phase of the microwave field within the cavity is independent of microwave power (as it should be). The second point to note is that the microwave phase can get relatively large when the real part of $H_z$ is sufficiently small, that is, when the Rabi frequency of the atom is sufficiently small. Inspection of (3) shows that this can happen whenever the real part of $H_z$ tends toward zero more rapidly than the imaginary part of $H_z$. This happens at the ends of the cavity in which the cavity phase near the endcaps may reach milliradians or more. For example, on the axis of the NIST-F1 cavity, just above the lower endcap at $z = 10^{-5}$ cm, according to (3), the cavity phase approaches 1 radian. However, the phase of the atomic wave function is affected only at the microradian level because the microwave field (and hence the atom's Rabi frequency) is $10^{-5}$ of its value at the center of the cavity. Because the Rabi frequency of the atom is (essentially) zero, the atom is (essentially) unaffected by the relatively large numerical value of the microwave phase. In other words, what is ultimately of interest is not the value of the phase angle of the microwave field, but rather the value of the phase angle imposed on the atomic wave function as a result. In order to quantify the effect of the imaginary part of the microwave field upon the atom, we now obtain a solution to the time-dependent Schrödinger equation as the atoms pass through a cavity with fields described by (2) and (4).

## III. Schrödinger Equation and Ramsey Lineshapes

We extensively use the theoretical framework developed by Shirley [16], [17] and Shirley *et al.* [18] and give here the extensions required to handle both the real and imaginary phases of the microwave field within the cavity.

We begin by assuming that the problem can be handled within the framework of a two-level system. The Hamiltonian for the system can be written as (cf. (7) of [18]):

$$H = \hbar \begin{pmatrix} \omega_a & 2b\cos\omega t + 2b'\sin\omega t \\ 2b\cos\omega t + 2b'\sin\omega t & \omega_b \end{pmatrix}, \tag{5}$$

where $\hbar\omega_a$ and $\hbar\omega_b$ are the energies of the upper and lower states, respectively. The interaction Rabi frequency for the real part of the microwave field is given by $2b = \mu_B g \mathrm{Re}\,(H_Z)/\hbar$ where $\mu_B$ is the Bohr magneton, $g$ is the Landé $g$-factor, and $H_Z$ is the microwave magnetic field parallel to the quantization axis imposed by the external C-field. A similar expression applies for $b'$, $2b' = \mu_B g \mathrm{Im}\,(H_Z)/\hbar$, the Rabi frequency due to the imaginary part of the microwave field. Both $b(t)$ and $b'(t)$ are time dependent, owing to the atom's motion in the cavity. We also define $b_0 \equiv (g\mu_B/2\hbar)\, H_0$.

In the rotating wave approximation, the Hamiltonian in (5) is written:

$$H = \hbar \begin{pmatrix} \omega_a & (b+ib')\, e^{-i\omega t} \\ (b-ib')\, e^{i\omega t} & \omega_b \end{pmatrix}. \tag{6}$$

Note the sign change in $b'(t)$ in the off-diagonal couplings. This comes about because the rotating-wave approximation selects one exponential from $\sin \omega t$ in one coupling and the other exponential in the other coupling (compare to (7) and (8) in [18]). Using the "phase factored" solutions, $\alpha$ and $\beta$, (cf (9) and (10) of [18]) gives us the Schrödinger equation for the system:

$$i\hbar \frac{d}{dt}\begin{pmatrix}\alpha \\ \beta\end{pmatrix} = \hbar \begin{pmatrix} -\Delta & (b+ib') \\ (b-ib') & \Delta \end{pmatrix}\begin{pmatrix}\alpha \\ \beta\end{pmatrix}, \tag{7}$$

where $\alpha$ is the probability amplitude that the system remains in its initial state, and $\beta$ is the probability amplitude that the system changes state. $\Delta$ is half the detuning $\delta\omega$ from the atomic resonance $\omega_0$; $\Delta = (1/2)(\omega - \omega_0) = (\delta\omega/2)$, where $\omega_0 = \omega_a - \omega_b$ is the hyperfine splitting of the atom. $\Delta$, $b$, and $b'$ are all real, possibly time-dependent, quantities.

We now give a solution to (7), valid through first order in $\Delta$ and $b'(t)$, under the assumption that the detuning is small compared to the Rabi frequency and that $\Delta$ is constant. $\alpha$ and $\beta$, obtained by analogy with (25)–(28) of [18], can be expressed as:

$$\begin{aligned} \alpha(\tau) &= \cos a(\tau) + i\Delta\zeta(\tau) - i\eta(\tau) \text{ and} \\ \beta(\tau) &= -i \sin a(\tau) - \Delta\xi(\tau) - \varepsilon(\tau), \end{aligned} \tag{8}$$

here $a$, $\zeta$, $\eta$, $\xi$, and $\varepsilon$ are given by:

$$\begin{aligned} a(t) &= \int_0^t b(t')\, dt' = \frac{b_0\tau}{2}\left[1 - \cos\left(\frac{\pi t}{\tau}\right)\right], \\ \zeta &= \int_0^\tau \cos(2a(t) - a(\tau))\, dt, \\ \eta &= \int_0^\tau b'(t) \sin(2a(t) - a(\tau))\, dt, \\ \xi &= \int_0^\tau \sin(2a(t) - a(\tau))\, dt, \text{ and} \\ \varepsilon &= \int_0^\tau b'(t) \cos(2a(t) - a(\tau))\, dt. \end{aligned} \tag{9}$$

Note that the first-order corrections, $\zeta$, $\eta$, $\xi$, $\varepsilon$, to $\alpha$ and $\beta$ are out of phase with the primary parts of $\alpha$ and $\beta$, and, hence, become of second order in the Rabi transition probability; but they affect the Ramsey fringe in first-order as shown below.

If we use subscripts 1 and 2 to denote the first and second Ramsey microwave interactions and denote the Ramsey drift time by $T_R$, the wave function for Ramsey excitation can be written as (compare (35) of [18]):

$$\begin{aligned} &\psi(\tau_2 + T_R + \tau_1) \\ &= \begin{pmatrix} \alpha_2 & -\beta_2^* \\ \beta_2 & \alpha_2^* \end{pmatrix} \begin{pmatrix} e^{i\delta\omega T_R/2} & 0 \\ 0 & e^{-i\delta\omega T_R/2} \end{pmatrix} \begin{pmatrix} \alpha_1 & -\beta_1^* \\ \beta_1 & \alpha_1^* \end{pmatrix} \psi(0), \end{aligned} \tag{10}$$

where $\psi(0)$ is given here by:

$$\psi(0) = \begin{pmatrix}\alpha(0) \\ \beta(0)\end{pmatrix} \equiv \begin{pmatrix}1 \\ 0\end{pmatrix}. \tag{11}$$

The transition amplitude from the initial state to the final state is given by:

$$\alpha_1\beta_2 e^{i\delta\omega T_R/2} + \alpha_2^*\beta_1 e^{-i\delta\omega T_R/2}, \tag{12}$$

and the transition probability is given by its absolute square:

$$P = |\alpha_2|^2 |\beta_1|^2 + |\alpha_1|^2 |\beta_2|^2 + 2\mathrm{Re}\left[\beta_2\beta_1^*\alpha_2\alpha_1 e^{i\delta\omega T_R}\right]. \tag{13}$$

Using our previous solutions (8) for $\alpha$ and $\beta$ and assuming that $a(\tau)$ is the same for both excitations leads to a transition probability of:

$$\begin{aligned} P = \frac{\sin^2(2a(\tau))}{2}\Bigg[1 + \cos\delta\omega T_R + \Bigg\{ &(\varepsilon_2 - \varepsilon_1)\csc a(\tau) \\ + \left((\eta_1 + \eta_2) - \frac{\delta\omega}{2}(\zeta_2 - \zeta_1)\right)\sec a(\tau)\Bigg\} \sin\delta\omega T_R\Bigg]. \end{aligned} \tag{14}$$

Only terms of zeroth and first order in $\varepsilon$, $\eta$, $\zeta$, and $\xi$ have been retained. $P$ can clearly be seen as a normal Ramsey fringe (the $\cos\delta\omega T_R$ term) plus an underlying fringe of small amplitude and $\pi/2$ displacement (the $\sin\delta\omega T_R$ term). The terms symmetric in the detuning, $\delta\omega$, (the $\cos\delta\omega$ and $(\delta\omega/2)(\zeta_2 - \zeta_1)\sin\delta\omega$ terms), do not lead to a frequency shift. The asymmetric terms, however, cause a distortion of the Ramsey curve and, therefore, lead to a frequency bias. When using square-wave frequency modulation, the frequency bias at optimum power is proportional to the difference in the transition probability on the left and right sides of the central Ramsey fringe at equal detunings. This difference is given by:

$$P_L - P_R = \sin^2(2a(\tau))\left[\frac{\varepsilon_2 - \varepsilon_1}{\sin(a(\tau))} + \frac{\eta_2 + \eta_1}{\cos(a(\tau))}\right], \tag{15}$$

where $P_{L,R}$ is the probability given by (14) on the left and right sides of the central Ramsey fringe, respectively (that is with $\delta\omega = \mp(\pi/2T_R)$, respectively); (15) is shown plotted below in Fig. 2. The corresponding (fractional) frequency shift:

$$\begin{aligned} \frac{\delta\nu}{\nu} &\simeq \frac{P_L - P_R}{\omega_0 T_R \sin^2(2a(\tau))} \\ &= \frac{1}{\omega_0 T_R}\left[\frac{\varepsilon_2 - \varepsilon_1}{\sin(a(\tau))} + \frac{\eta_2 + \eta_1}{\cos(a(\tau))}\right], \end{aligned} \tag{16}$$

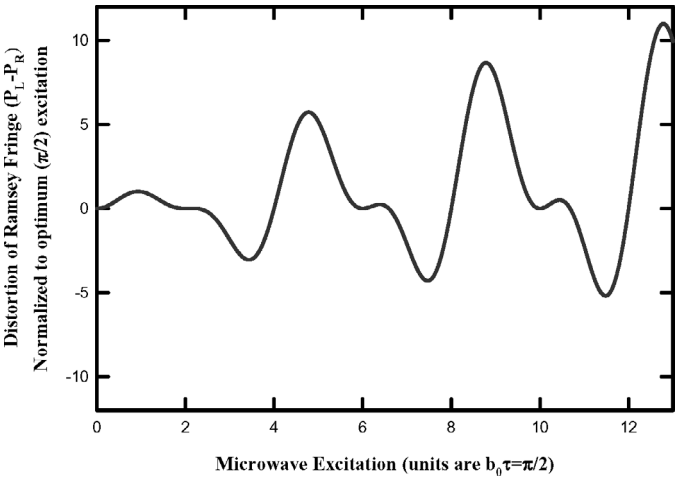


Fig. 2. The calculated microwave power dependence of the distortion of the central Ramsey fringe caused by the distributed cavity phase shift. The calculation is normalized to the shift at optimum ($\pi/2$) power.

is given by (15) divided by twice the slope of the side of the Ramsey fringe. As we shall see later, $\eta_1$ and $\eta_2$ are zero in the present case. Furthermore, (16) becomes singular when $a(\tau) = \pi$, $2\pi$, $3\pi$, etc. This singularity in the frequency shift is perfectly acceptable; it happens when the transition probability (14) vanishes. And (16) applies when using normal, slow-square-wave frequency modulation, but the result for slow-square-wave phase modulation is similar.

## IV. Power Dependence

We approximate $b'(t)$ with the leading radial term in (4) (because of the time-reversal symmetry experienced by an atom in a fountain trajectory, the constant term does not cause a frequency shift in a fountain) to get:

$$\eta_{1,2} = \frac{b_0\pi}{2Q}\int_0^\tau \left(\frac{\rho_{1,2}}{r_C}\right)^2 \left(\frac{z}{d}-\frac{1}{2}\right)^2 \sin\left(b_0\tau\cos\left(\frac{\pi t}{\tau}\right)\right)\,dt, \tag{17}$$

$$\varepsilon_{1,2} = \frac{b_0\pi}{2Q}\int_0^\tau \left(\frac{\rho_{1,2}}{r_C}\right)^2 \left(\frac{z}{d}-\frac{1}{2}\right)^2 \cos\left(b_0\tau\cos\left(\frac{\pi t}{\tau}\right)\right)\,dt,$$

where $\eta_{1,2}$ or $\varepsilon_{1,2}$ denotes $\eta$ or $\varepsilon$ on the first or second pass through the cavity, as appropriate, and similarly for $\rho_{1,2}$. The $\eta_{1,2}$ term vanishes identically from symmetry considerations. The evaluation of $\varepsilon_{1,2}$ is facilitated by the identity (9.1.44 in [19]):

$$\cos(\gamma\cos\theta) = J_0(\gamma) + 2\sum_k (-1)^k J_{2k}(\gamma)\cos(2k\theta). \tag{18}$$

This can be substituted into (17) along with the replacement of $z/d$ by $t/\tau$, and assuming vertical atom-trajectories ($\rho_{1,2}$ constant over one pass through the cavity) to give:

$$\varepsilon_{1,2} = \frac{b_0\pi}{2Q}\left(\frac{\rho_{1,2}}{r_C}\right)^2 \int_0^\tau \left(\frac{t}{\tau}-\frac{1}{2}\right)^2 \left[J_0(b_0\tau) + 2\sum_{k=1}^{\infty}(-1)^k J_{2k}(b_0\tau)\cos\left(2k\frac{\pi t}{\tau}\right)\right] dt. \tag{19}$$

Evaluating $\varepsilon_{1,2}$ (19), we find:

$$\varepsilon_{1,2} = \frac{\pi b_0\tau}{24Q}\left(\frac{\rho_{1,2}}{r_C}\right)^2 \left[J_0(b_0\tau) + \frac{12}{\pi^2}\sum_{k=1}^{\infty}\frac{(-1)^k}{k^2}J_{2k}(b_0\tau)\right], \tag{20}$$

where the power dependence is now explicit in $b_0\tau$.

We now take the simplified case of $\rho_1 = 0$ and $\rho_2 = (r_C/6)$), corresponding to the atom ascending on the centerline of the cavity and descending just next to the wall of the below-cutoff waveguide in our cavity. The Ramsey microwave cavity in NIST-F1 has an unloaded $Q$ of 22,500 and a cavity radius, $r_C$, of 3.0 cm, and is resonant at 9.1926 GHz, which we use for the analysis here [10]. The distortion of the Ramsey fringe by the distributed cavity phase as a function of microwave power (15) is shown in Fig. 2, and the frequency bias caused by the distributed cavity phase (16) is given in Table I.

TABLE I
Microwave Field Dependence of the Frequency Bias Attributable to Distributed Cavity Phase.

| Microwave field amplitude, $b_0\tau = (n\pi/2)$[1] | Frequency shift, normalized to the frequency shift at $b_0\tau = (\pi/2)\cdot\left[\frac{\delta\nu@(n\pi/2)}{\delta\nu@(\pi/2)}\right]$ |
|---|---|
| $n = 1$ | 1 |
| $n = 3$ | −1.855 |
| $n = 5$ | 5.169 |
| $n = 7$ | −2.129 |
| $n = 9$ | 7.832 |
| $n = 11$ | −2.254 |
| $n = 13$ | 9.957 |

[1]The microwave field is given in units of $\pi/2$ pulses where $b_0\tau = (n\pi/2)$.

It clearly can be seen from Fig. 2 and the data in Table I that the frequency bias caused by the distributed cavity phase is a function of microwave power. For example, the frequency shift between excitations of $3\pi/2$ and $5\pi/2$ caused by the distributed cavity phase shift is approximately seven times larger than the shift at optimum excitation. This dependence on microwave power allows the frequency bias from the distributed cavity phase to be measured, or at least constrained. Note also that the data in Fig. 2 and Table I are normalized to the shift at optimum power $b_0\tau = (\pi/2)$.

The results plotted in Fig. 2 and given in Table I are not critically dependent on the exact form of the distributed

cavity phase assumed in (4). One way to deduce this is that what appears in the frequency shift (16) is the integral of $b'$ weighted by $b$, an average of $b'$ that is relatively insensitive to the details of $b'$. If, however, the imaginary part of the microwave field is assumed to have the same spatial dependence as the real part of the microwave field, the power dependence of $\varepsilon$ cancels that in (16). This is as it should be. If the imaginary and real parts of the field have the same spatial dependence, then the distributed cavity phase is constant (3), and the frequency shift vanishes exactly. In fact, the power dependence exists whenever the temporal dependance (as seen by the atoms) of the real and imaginary parts of the field are different, which they will be in any cavity with below cutoff waveguides in the endcaps.

Although we have evaluated the shift for a "worst case" atom trajectory, the shape of the shift as shown in Fig. 2 (and given in Table I) is invariant for other trajectories (up to a factor of $-1$) with the assumption that the atom travels vertically on a single pass through the cavity. The overall frequency bias in the fountain then is given by evaluating the bias over the atomic distribution function.

## V. Discussion

The frequency shifts associated with microwave leakage are closely related to the frequency shifts associated with distributed cavity phase. In both cases, the frequency shift is associated with an out-of-phase excitation, which is inside the cavity for the case of the distributed cavity phase bias and between the cavities in the case of frequency bias from microwave leakage. Impurities in the microwave spectrum also give rise to frequency biases that are dependent on the microwave power level. As a result of the relatively complicated signature of the distributed cavity phase-shift frequency bias with microwave power, it may be possible to separate the effects of leakage, microwave spectrum, and distributed cavity phase by measuring the frequency bias at several microwave powers. This will require a theory of the effects of microwave leakage more complete than currently exists in the literature. Until we have a complete theory of the dependence on power of the frequency biases associated with:

- microwave leakage,
- the microwave spectrum, and
- distributed cavity phase,

the frequency biases which have been attributed to each of these effects are in some doubt. We are presently developing a more complete theory of the microwave leakage at elevated microwave power.

We have measured the microwave power dependence of the output frequency of NIST-F1 many times and have not seen a statistically significant shift. Using data from these measurements and assuming that the frequency bias from the distributed cavity phase is the dominant effect (which we believe to be the case), the frequency bias attributable to the distributed cavity phase shift in NIST-F1 at optimum excitation is no more than $(\delta f/f) \leq 1\times10^{-16}$.

Most laboratories operating cesium fountain primary-frequency standards test for a microwave leakage bias by using elevated microwave power in their standards [20]–[23]. It usually is assumed during these tests that the frequency bias associated with the distributed cavity phase is invariant under changes in microwave power. However, it can be seen from Fig. 2 and Table I that these tests may significantly alter any frequency shift due to the distributed cavity phase. High-power microwave tests in a fountain with a significant distributed cavity phase induced-frequency bias can lead to mistakes in estimating both the sign and magnitude of the leakage bias if that frequency bias is assumed to be linear in the microwave field amplitude. Consider a fountain in which the leakage bias at high microwave powers is estimated by measuring the frequency shift when operated at $3\pi/2$ and $7\pi/2$, then using Table I we see that the shifts from distributed cavity phase measured are of opposite sign to the shift at $\pi/2$, and the magnitude of the bias also never approaches the factor of 7 one would assume from linearity.

In a typical case, for example, the frequency bias associated with microwave leakage was quoted as $(\delta f/f) \leq 2.0 \times 10^{-16}$ as evaluated by high-power microwave tests, and the frequency bias associated with the distributed cavity phase was theoretically evaluated as $(\delta f/f) \leq 1\times10^{-15}$ and both effects were included in the uncertainty analysis [23].

It is reasonable to conclude in this case that the bias from the cavity phase was already counted, at least partially, in the microwave leakage experiment and should not be counted again in a theoretical evaluation. If the bias from the distributed cavity phase shift is constrained by measurement to a value smaller than that from a theoretical simulation of the cavity, it seems that the measured constraint is the appropriate one to use.

## Appendix A
## The Bloch Vector Approach: An Alternative Viewpoint

In a classic paper, Rabi *et al.* [24] formulated the solution of Schrödinger's equation as the precession of a magnet in a magnetic field (the "Bloch vector") [24]. Feynman *et al.* [25] later reinterpreted the result more generally, and we use their formulation here. The wave function of any cesium atom in the fountain may be written as:

$$\psi(t) = \alpha(t)\psi_\alpha + \beta(t)\psi_\beta, \tag{21}$$

where $\psi_\alpha$ and $\psi_\beta$ are the eigenstates of the two-level system of interest here. Following [25], we define the components of a "spin vector" in a rotating frame:

$$\begin{aligned} r_1 &\equiv \alpha\beta^* + \beta\alpha^*, \\ r_2 &\equiv i\left(\alpha\beta^* - \beta\alpha^*\right), \\ r_3 &\equiv \alpha\alpha^* - \beta\beta^*. \end{aligned} \tag{22}$$

Direct substitution of (7) into (22) gives the equation of motion of the spin vector in an external field, including the imaginary part of the microwave field. We find the motion of the spin vector is described by:

$$\begin{aligned}\dot{r}_1 &= \delta\omega r_2 - 2b' r_3,\\ \dot{r}_2 &= -\delta\omega r_1 - 2b r_3,\\ \dot{r}_3 &= 2b r_2 + 2b' r_1.\end{aligned} \tag{23}$$

And (23) preserves the normalization $r_1^2 + r_2^2 + r_3^2 = 1$. In this picture, the probability that the atom be in state $\beta$ is given by $P_\beta = 1/2\ (1 - r_3)$.

We have numerically integrated (23) over a complete Ramsey-style excitation starting in state $\alpha$, (11), and using the microwave fields in (2) and (4). The resulting data for the probability that the atom is in state $\beta$ then is used to calculate the distortion in the Ramsey fringe at $\delta\omega = \mp(\pi/2T_R)$. This numerical approach reproduces the data shown in Fig. 2 with a root mean square error of less than 1%. The close agreement of the numerical result with the analytic result (16) and (15) provides strong confirmation of the analytic result.

Expression (23) also can be solved analytically, to the order of approximation in this paper, giving a result for the transition probability that is of a slightly simpler form than given in (14), but which is identical to it. We outline the method here.

The state of the atomic system upon beginning the first pass through the cavity is assumed to be described by $r_1 = r_2 = 0$, and $r_3 = 1$, (11). An approximate solution is first obtained by neglecting terms in $\Delta$ and $b'(t)$. The result is $r_2 = -\sin 2a(t)$, $r_3 = \cos 2a(t)$. Substituting back into the first of the equations of motion and integrating gives to first order:

$$r_1(t) = -2\Delta \int_0^t \sin\left(2a\left(t'\right)\right)\, dt' - 2\int_0^t b'\left(t'\right)\cos\left(2a\left(t'\right)\right) dt'. \tag{24}$$

Then because $r_1$ is of first order, no further changes in the other components are required.

As the atom passes into the drift region, boundary values of the spin components must be matched. Thus at $t = \tau_1$, the boundary conditions are:

$$r_{11} = r_1\left(\tau_1\right),\ r_2 = -\sin\left(2a_1\right),\ r_3 = \cos\left(2a_1\right). \tag{25}$$

Because there are no significant microwave magnetic fields in the drift region, $r_1$ and $r_2$ oscillate harmonically. We temporarily take $t = 0$ at the boundary. Then solutions that satisfy the boundary conditions at $t = 0$ are:

$$\begin{aligned}r_1 &= -\sin\left(2a_1\right)\sin\left(2\Delta t + \varphi\right),\\ r_2 &= -\sin\left(2a_1\right)\cos\left(2\Delta t + \varphi\right),\\ r_3 &= \cos\left(2a_1\right),\end{aligned} \tag{26}$$

where the phase $\varphi$ is determined by:

$$\sin\varphi = \frac{-r_{11}}{\sin\left(2a_1\right)}, \tag{27}$$

and terms in the square of $r_{11}$ are ignored. The components at the boundary between leaving the drift region and the second pass through the cavity are obtained from (26) by substituting $t = T_R$. And (26) then become boundary conditions for the components on the second pass. In particular we set:

$$r_{12} = -\sin\left(2a_1\right)\sin\left(2\Delta T_R + \varphi\right). \tag{28}$$

We can obtain an approximate solution of the equations of motion in the second passage through the cavity by again neglecting terms in $\Delta$ and $b'$. The results can be expressed as:

$$\begin{aligned}r_1 &= r_{12} = \sin B,\\ r_2 &= \cos B\cos\left(2a(t) + C\right),\\ r_3 &= \cos B\sin\left(2a(t) + C\right),\end{aligned} \tag{29}$$

where $C$ is an integration constant, and where we take $t = 0$ at the instant the atom starts the second pass through the cavity. The constant $C$ is determined from the boundary conditions:

$$\begin{aligned}\cos C &= -\frac{\sin\left(2a_1\right)\cos\left(2\Delta T_R + \varphi\right)}{\cos B},\\ \sin C &= \frac{\cos\left(2a_1\right)}{\cos B}.\end{aligned} \tag{30}$$

A first order solution to the equations of motion now can be obtained by the method of variation of constants—that is, we let $B$ and $C$ vary with time and substitute the solutions, (29), into the equations of motion and differentiate, keeping only first-order terms in $\Delta$ and $b'$. (Only two independent quantities vary because of normalization.) The equations can be combined to give:

$$\begin{aligned}\dot{B} &= 2\Delta\cos\left(2a + C\right) - 2b'\sin\left(2a + C\right),\\ \dot{C} &= \tan B\left[2\Delta\sin\left(2a + C\right) + 2b'\cos\left(2a + C\right)\right].\end{aligned} \tag{31}$$

On the right, the quantities $B$ and $C$ can be taken to be constants, to the order of the calculation. Then (31) can be integrated. The results are given by (32) (see next page).

The final transition probability now can be constructed using the expression for probability in terms of $r_3$, and (29), (30), and (32), and expanding all terms only to first order in the small quantities $\Delta$ and $b'$. The result is of the same form as (14), except that the coefficient of the $\sin\left(\delta\omega T_R\right)$ term inside the brackets is (33) (see next page) where $b_1$ and $b_2$ are $b'$ on the first and second passes through the Ramsey cavity. The result is identical to (14), but the integrations occur in a somewhat simpler form.

## Acknowledgments

The authors are pleased to acknowledge many useful discussions of microwave field effects in primary frequency standards with Andrea DeMarchi, Bob Drullinger, Bill Klipstein, Stefania Romisch, Tom Heavner, Elizabeth

$$C(t) = C + \tan B \left[ 2\Delta \int_0^t \sin\left(2a\left(t'\right) + C\right) dt' + 2 \int_0^t b'\left(t'\right) \cos\left(2a\left(t'\right) + C\right) dt' \right],$$
$$\cos B(t) = \cos B - \sin B \left[ 2\Delta \int_0^t \cos\left(2a\left(t'\right) + C\right) dt' + 2 \int_0^t b'\left(t'\right) \sin\left(2a\left(t'\right) + C\right) dt' \right]. \tag{32}$$

$$\left\{ \begin{array}{l} -2\Delta \int_0^\tau \sin\left(2a\left(t'\right)\right) dt' \dfrac{1-\cos 2a}{\sin 2a} - 2\Delta \int_0^\tau \cos\left(2a\left(t'\right)\right) dt' \\ -2 \int_0^\tau b_1\left(t'\right) \cos\left(2a\left(t'\right)\right) dt' / \sin 2a + 2 \int_0^\tau b_2\left(t'\right) \sin\left(2a\left(t'\right)\right) dt' \\ +2 \int_0^\tau b_2\left(t'\right) \cos\left(2a\left(t'\right)\right) dt' \dfrac{\cos 2a}{\sin 2a}. \end{array} \right\}. \tag{33}$$

Donley, Filippo Levi, and Tom Parker. We also thank the reviewers for their thoughtful comments that greatly improved the paper.

## References


[1] N. Ramsey, *Molecular Beams*. Oxford: Clarendon, 1956.

[2] R. C. Mockler, "Atomic beam frequency standards," *Adv. Electron El. Phys.*, vol. 15, pp. 1–72, 1962.

[3] S. Jarvis, Jr., "Molecular beam tube frequency biases due to distributed cavity phase variations," NBS Technical Note 660, Boulder, CO: U.S. Department of Commerce, Time and Frequency Division, National Bureau of Standards, 1975.

[4] A. DeMarchi, J. H. Shirley, D. J. Glaze, and R. E. Drullinger, "A new cavity configuration for cesium beam primary frequency standards," *IEEE Trans. Instrum. Meas.*, vol. 37, pp. 185–190, 1988.

[5] A. Bauch, B. Fischer, T. Heindorff, and R. Schröder, "Performance of the PTB reconstructed primary clock CS1 and an estimate of its current uncertainty," *Metrologia*, vol. 35, pp. 829–845, 1998.

[6] M. Abgrall, "Evaluation des performances de la fontaine atomique PHARAO, participation à l'étude l'horloge spatiale PHARAO," Ph.D. dissertation, University de Paris VI, Jan. 2003.

[7] A. DeMarchi, "The optically pumped caesium fountain: $10^{-15}$ frequency accuracy?," *Metrologia*, vol. 18, pp. 103–116, 1982.

[8] G. Vecchi and A. DeMarchi, "Spatial phase variations in a $TE_{011}$ microwave cavity for use in a cesium fountain primary frequency standard," *IEEE Trans. Instrum. Meas.*, vol. 42, pp. 434–438, 1993.

[9] A. Khursheed, G. Vecchi, and A. DeMarchi, "Spatial variations of field polarization in microwave cavities: Application to the cesium fountain cavity," *IEEE Trans. Ultrason., Ferroelect., Freq. Contr.*, vol. 43, pp. 201–210, 1996.

[10] S. R. Jefferts, R. E. Drullinger, and A. DeMarchi, "NIST cesium fountain microwave cavities," in *Proc. Int. Freq. Contr. Symp.*, 1998, pp. 6–8.

[11] P. Laurent, P. Lemonde, M. Abgrall, G. Santarelli, F. Pereira Dos Santos, A. Clairon, P. Petit, and M. Aubourg, "Interrogation of cold atoms in a primary frequency standard," in *Proc. Joint Mtg. IEEE Int. Freq. Contr. Symp. and EFTF Conf.*, 1999, pp. 152–155.

[12] C. Fertig, R. Li, J. Rees, and K. Gibble, "Distributed cavity phase shifts and microwave photon recoils," in *Proc. IEEE Int. Freq. Contr. Symp.*, 2002, pp. 469–472.

[13] G. J. Dick, W. M. Klipstein, T. P. Heavner, and S. R. Jefferts, "Design concept for the microwave interrogation structure in PARCS," in *Proc. Joint Mtg. IEEE Int. Freq. Contr. Symp. and EFTF Conf.*, 2003, pp. 1032–1036.

[14] N. Ashby, S. Römisch, and S. R. Jefferts, "Endcaps for $TE_{011}$ cavities in fountain frequency standards," in *Proc. Joint Mtg. IEEE Int. Freq. Contr. Symp. and EFTF Conf.*, 2003, pp. 1076–1083.

[15] R. E. Collin, *Foundations of Microwave Engineering*. 2nd ed. New York: McGraw-Hill, 1998.

[16] J. H. Shirley, "Some causes of resonant frequency shifts in atomic beam machines I. Shifts due to other frequencies of excitation," *J. Appl. Phys.*, vol. 34, pp. 783–788, 1963.

[17] J. H. Shirley, "Solution of the Schrödinger equation with a Hamiltonian periodic in time," *Phys. Rev.*, vol. 138, pp. B979–B987, 1965.

[18] J. H. Shirley, W. D. Lee, and R. E. Drullinger, "Accuracy evaluation of the frequency standard NIST-7," *Metrologia*, vol. 38, pp. 427–458, 2001.

[19] M. Abramowitz and I. E. Stegun, *Handbook of Mathematical Functions*. Washington, DC: United States Department of Commerce, National Bureau of Standards, ser. Applied Mathematics Series 55, 1964.

[20] S. R. Jefferts, J. H. Shirley, T. E. Parker, T. P. Heavner, D. M. Meekhof, C. W. Nelson, F. Levi, G. Costanzo, A. DeMarchi, R. E. Drullinger, L. Hollberg, W. D. Lee, and F. L. Walls, "Accuracy evaluation of NIST-F1," *Metrologia*, vol. 39, pp. 321–336, 2002.

[21] S. Weyers, U. Hübner, R. Schröder, C. Tamm, and A. Bauch, "Uncertainty evaluation of the atomic caesium fountain CSF1 of the PTB," *Metrologia*, vol. 38, pp. 343–352, 2001.

[22] F. Levi, L. Lorini, D. Calonico, and A. Godone, "IEN-CSF1 accuracy evaluation and two-way frequency comparison," *IEEE Trans. Ultrason., Ferroelect., Freq. Contr.*, vol. 51, no. 10, pp. 1216–1224, Oct. 2004.

[23] A. Clairon, S. Ghezali, G. Santarelli, Ph. Laurent, S. N. Lea, M. Bahoura, E. Simon, S. Weyers, and K. Szymaniec, "Preliminary accuracy evaluation of a cesium fountain frequency standard," in *Proc. 5th Symp. Freq. Standards Metrology*, 1995, pp. 49–59.

[24] I. I. Rabi, N. F. Ramsey, and J. Schwinger, "Use of rotating coordinates in magnetic resonance problems," *Rev. Mod. Phys.*, vol. 26, pp. 167–171, 1954.

[25] R. P. Feynman, F. L. Veron, and R. W. Hellwarth, "Geometrical representation of the Schrödinger equation for solving maser problems," *J. Appl. Phys.*, vol. 28, pp. 49–52, 1957.

**Steven R. Jefferts** (M'01) received a B.S. degree in Physics from the University of Washington in Seattle, WA, in 1984 and a Ph.D. in atomic physics/precision metrology from JILA/University of Colorado in Boulder, CO, in 1992. His thesis work involved ultra-high precision mass spectroscopy of light ions.

He then went "across the street" to NIST as an NRC postdoctoral fellow working with Dave Wineland on laser-cooled trapped ions.

In 1994 he joined the Time and Frequency division of the National Institute of Standards and Technology (NIST) as a permanent employee. Dr. Jefferts leads the research group developing and operating cesium fountain primary frequency standards.

Dr. Jefferts received the Edward Uhler Condon award in 2001, a Department of Commerce Gold metal in 2004, and the Arthur S. Flemming award in 2005. He was also the IEEE-UFFC distinguished lecturer for 2003–2004.

**Jon H. Shirley** was born in Minneapolis, MN in 1936. He received a B.A. from Middlebury College in 1957 and Ph.D. from California Institute of Technology in 1963. For many years he was a physicist at the National Bureau of Standards in Boulder, CO. He performed theoretical studies of the resonant interaction of radiation with atoms. In 1975–1976, he spent a year at the University of Helsinki in Finland. He received the I. I. Rabi Award at the 2002 IEEE International Frequency Control Symposium. Currently he is a consultant to the Time and Frequency Division at the National Institutes of Standards and Technology in Boulder, CO. His principal effort is the determination of biases that affect the U.S. primary frequency standard.

**Neil Ashby** is Professor of Physics Emeritus at the University of Colorado and a Staff Scientist at the National Institute of Standards and Technology (NIST) at Boulder, CO. Prof. Ashby is involved with theoretical studies of general relativity and its practical applications. He has written extensively on the role of relativity in celestial navigation. His applied-relativity projects include the study of relativistic effects in the network of satellites that form the Global Positioning System and relativity corrections to the trajectories of planets and orbiting satellites. Prof. Ashby currently works at NIST on applications of relativity to clocks, the use of atomic clocks for advanced navigation concepts, and for testing relativity. He is also a "Mentor" to about 30 graduate students and post-docs who work at NIST but who are from University of Colorado.

**Eric A. Burt** was born in Berkeley, California in 1957. He received a B.S. degree with honors in mathematics from the University of Michigan, Ann Arbor, MI, in 1979, a M.S. degree in physics from the University of Washington, Seattle, WA, in 1990 and a Ph.D. in physics from the University of Washington in 1995. His Ph.D. was in experimental atomic physics working with trapped laser-cooled single ions. After receiving his Ph.D. in physics he worked at the University of Colorado, in Boulder, CO, from 1995 to 1997 on experiments with Bose-Einstein condensates. There he performed the first experiment to demonstrate higher-order (laser-like) coherence in condensate atoms. From 1997 to 2001 he worked at the U.S. Naval Observatory in Washington, D.C., developing a cesium fountain atomic clock. From 2001 to the present he has worked at the Jet Propulsion Laboratory, Pasadena, CA, on the development of both ion and laser-cooled neutral atomic clocks. Dr. Burt is a member of the American Physical Society and the IEEE.

**G. John Dick** was born in 1939 in Ohio. He received his A.B. in physics and mathematics from Bethel College, Kansas, in 1961 and a Ph.D. degree in physics from the University of California-Berkeley in 1969.

After a postdoctoral fellowship at Caltech, he joined the research faculty there as senior research fellow, developing RF resonator technology for superconducting accelerator applications. During 1979-1980 he also was appointed as a visiting faculty member at SUNY Stonybrook in New York. In 1986 he joined the staff of the Jet Propulsion Laboratory, where he is presently a principal member of the technical staff. Duties include development of cryogenic sapphire oscillators (10 K CSO) presently under construction for installation in NASA's Deep Space Network, and project scientis responsible for SUMO, a superconducting microwave oscillator experiment scheduled for the second flight of the Low Temperature Microgravity Physics Facility (LTMPF) aboard the International Space Station.

His research interests include high-Q cryogenic resonator design and atomic frequency standard systematics. In April 1999 he was awarded "Le Prix European Temps-Frequence," presented at the joint meeting of the 13th European Frequency and Time Forum and the 1999 IEEE Intenational Frequency Control Symposium. The award is granted every 2 years by the Societe Française de Microtechniques et de Chronometrie to an individual or group for "degree of initiative and creativity, quality of work, degree of success obtained and worldwide impact on the Time and Frequency associated community."